Academic Journal of Science and Technology
ISSN: 2771-3032 | Vol. 14, No. 3, 2025

Study on the Properties of Alkali-activated Gold Tailings 3D Printing Concrete

Depeng Wang[1, *]

[1] School of Civil Engineering, Henan Polytechnic University, Jiaozuo 454000, China
[*] Corresponding author: Depeng Wang (Email: lsp547@126.com)

Abstract: The activity of gold tailings was activated by alkali activation method. Cement and gold tailings were used as cementitious materials to prepare 3D printing concrete. The mechanical properties and rheological characteristics of the slurry were measured to evaluate its performance during 3D printing. The results showed that when the content of gold tailings was approximately 1:1 with the amount of cement, the 28-day strength reached 31.9MPa, and the concrete had the best performance during 3D printing. The lateral deflection of the cylindrical components printed with gold tailings concrete was more than 50% lower than that of traditional concrete, the structural integrity was higher, and the printing open time was within a reasonable range.

Keywords: 3D Concrete Printing; Gold Tailings; Alkali Activation; Rheological Properties.

1. Introduction

Tailings are waste products generated during the mining process. Long-term accumulation of tailings has caused great occupation and pollution of land. In the rainy season, tailings ponds may also cause geological secondary disasters such as landslides due to the flow of surface water [1], and even there is a risk of tailings pond dam collapse. The storage and preservation of tailings also increase the operating costs of mining enterprises [2]. In terms of tailings reuse, tailings are used as raw materials to prepare filling paste, which is filled into goafs to prevent mine surface collapse and subsidence [3]. Or tailings are reused in building materials, such as being mixed into clay brick materials for sintering [4]. High-temperature calcination can stimulate the potential pozzolanic activity of tailings [5]. The practical application of tailings has relevant examples and has achieved good application benefits. Gold mining produces a large amount of gold tailings, which contain a large number of aluminum-silicon oxides such as SiO_2, Fe_2O_3, and Al_2O_3 [6]. During the alkali activation treatment, the crystal structure of part of the gold tailings is destroyed, generating more amorphous active silica, thereby improving the activity of the tailings [7-8], which points out a new direction for the solid waste reuse of gold tailings [9].

In terms of environmental protection, the comprehensive utilization of tailings solid waste has made great progress. With the increasing requirements for environmental protection, the construction field is also transforming towards the application of new technologies. 3D concrete printing (3DCP) is an innovative technology in the current construction field. Through the layer-by-layer stacking and curing of concrete materials, it realizes the rapid forming of buildings. Compared with traditional construction methods, 3DCP has many advantages such as material saving, construction period shortening, and construction efficiency improvement [10]. However, due to its special layer-by-layer stacking construction process, 3DCP technology relies on the force generated by the 3DCP concrete itself to maintain its shape to resist the upper load after stacking [11]. Based on the concept of rheology, the faster the strength growth rate of the slurry, the stronger the bearing capacity it can provide [12]. However, too fast strength growth rate limits the printability and printing open time of the material [13-15]. With the gradual in-depth research on alkali-activated cementitious materials, the use of alkali activation can effectively improve the early strength of the concrete slurry mixed with gold tailings, which has an excellent contribution to the early mechanical properties of the printed components [16]. As the proportion of alkali-activated gold tailings replacing fine aggregate increases, the initial and final setting times of 3DCP concrete decrease, and the fluidity and slump also decrease significantly, which can effectively regulate the rheological properties of 3DCP slurry and reduce the structural deformation during printing [17]. In addition, compared with traditional concrete, tailings-activated concrete can replace part of the cement in the concrete. Under the same strength, it can effectively reduce cement consumption, reduce the expansion of concrete defects and cracks [18], and effectively solidify heavy metals in tailings to prevent the leaching of heavy metal ions from damaging the natural environment [19].

At present, the research on alkali activation of gold tailings at home and abroad has not been widely applied in 3DCP technology. The utilization of gold tailings effectively reduces the economic loss and environmental damage caused by storage and transportation, and also fits the green, low-carbon and environmental protection technical concept of 3DCP technology [20]. For 3DCP technology, the extrudability of the material, appropriate printing open time, and buildability determine the quality of the printed components [21]. Using alkali activation technology can better adjust the fluidity and yield stress of the slurry. In order to enable gold tailings to effectively adjust the fluidity of 3DCP slurry, sodium hydroxide and sodium silicate are used to activate gold tailings to make it have high cementitious activity [22-23], and finally can replace part of the cement in 3DCP slurry to enhance the advantages of green, environmental protection, economy and efficiency of gold tailings concrete materials. In order to explore the rheological regulation effect of alkali activation of gold tailings on 3D printing slurry, based on the existing theoretical model of printing height [24-25], this paper quantitatively characterizes the contribution of gold tailings replacing cement to mechanics and fluidity, and

evaluates the cementitious effect and the contribution to improving printing quality generated after the activation of gold tailings.

2. Experimental Objectives and Scheme Design

2.1. Experimental Materials

Cement: The cement used in this experiment was P.O. 42.5 cement produced by a certain factory. The specific surface area of the cement was 401m²/kg, and the specific gravity was 3.15. XRF analysis was carried out on its contents, and the chemical composition results are shown in Table 1.

Table 1. Chemical Composition of Cement

Component	CaO	SiO_2	Al_2O_3	Fe_2O_3	SO_3
wt%	58.27	23.65	4.68	2.43	2.35

Fly Ash: F-grade fly ash was used, with an apparent density of 1.94g/cm³. After XRF determination, the mass fraction of SiO_2 in it was 53.45%, and Al_2O_3 accounted for 31.07%. It can also provide a certain amount of excitation products during the alkali activation process. Therefore, the mix proportion of this experiment will fix the fly ash content and evaluate the contribution of gold tailings and alkali activation to 3DCP slurry.

Table 2. Chemical Composition of Fly Ash

Component	SiO_2	Al_2O_3	Fe_2O_3	CaO	MgO
wt%	53.45	31.07	3.35	4.83	1.16

Gold Tailings: The gold tailings used in this experiment were by-products of a gold mine production process, separated by a deep cone thickener, and then dried and ground for measurement and experiment. The measured apparent density was 2814kg/m³, the bulk density was 1145kg/m³, and the mud content was 3.8%. The particle size distribution measured by a laser particle size analyzer is shown in Figure 1. It can be seen that the gold tailings after ball milling are relatively fine, and the proportion of particles smaller than 20μm is close to 50%. The mix proportion needs to be designed according to the fineness. XRF analysis of the gold tailings sample gives the chemical composition of gold tailings as shown in Table 3.

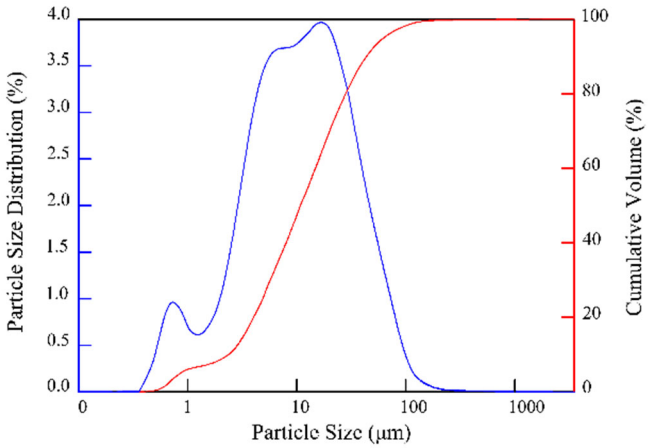

Figure 1. Particle Size Distribution of Gold Tailings

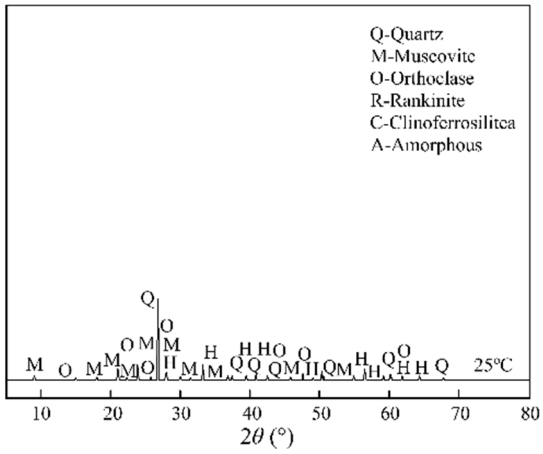

Figure 2. XRD Pattern of Gold Tailings at 25℃

Table 3. Chemical Composition of Gold Tailings

Component	SiO_2	Al_2O_3	CaO	Fe_2O_3	MgO
wt%	54.8	19.7	10.4	8.5	3.7

Fine Aggregate: River sand was used as the fine aggregate in the concrete. The river sand was dried before the experiment. The measured apparent density of the river sand was 2751kg/m³, the bulk density was 1672kg/m³, the water absorption was 2.3%, and the particle size gradation was in the range of 0.1mm-1.5mm.

Admixtures: Thickeners and water reducers were mainly used as admixtures to regulate the fluidity and cohesiveness of concrete. Hydroxypropyl methylcellulose (HPMC) was selected as the thickener, and polycarboxylate superplasticizer (PCE) was selected as the water reducer.

Alkali Activators: Sodium hydroxide and sodium silicate solution were selected as the alkali activators. Sodium hydroxide was a solid white particle with a purity of 97%. Sodium silicate was a liquid reagent with a modulus of 3.1 and a water content of 60%. The modulus of the alkali activator used in the experiment was 1.5. After preparing the alkali activator, it was necessary to use an ultrasonic cleaner for normal temperature water bath to ensure that the added sodium hydroxide was completely dissolved.

2.2. Mix Design

The 3DCP mix proportion used in this study was derived from previous research of our team, as shown in Table 4. A constant amount of hydroxypropyl methylcellulose thickener (HPMC) and polycarboxylate superplasticizer (PCE) were used in the mix proportion to enhance its fluidity and cohesiveness. The model printed with this mix proportion was selected because it had good appearance characteristics and could obtain better mechanical properties.

Table 4. Chemical Composition of Cement

Group	Cement (kg/m³)	Fly Ash (kg/m³)	Fine Aggregate (kg/m³)	Gold Tailings (kg/m³)	HPMC(g)	PCE(g)	Water (kg/m³)
T0	635	126	1083	0	1905	2540	203.2
T1	527	126	1083	108	1905	2540	203.2
T2	419	126	1083	216	1905	2540	203.2
T3	311	126	1083	324	1905	2540	203.2
T4	203	126	1083	432	1905	2540	203.2

2.3. Experimental Scheme and Equipment

2.3.1. Mechanical Properties and Setting Time Test

The raw materials required for the 3DCP concrete mix proportion in Table 4 were put into a mortar mixer, dry-mixed for 1min to make them fully mixed, then the prepared alkali activator and the required amount of water were added, and mixed for another 2min. Then it was poured into 100mm×100mm×100mm standard cube specimens, cured at room temperature for 24h and demolded, and then placed in a standard curing room. When cured for 3d and 28d, the compressive strength of the material was measured respectively, and the final result was the average of the measured results. At the same time, the Vicat apparatus was used to determine the initial setting time of the material to ensure that the initial setting time of the material was greater than the open time required for 3D printing, so as to ensure the continuity and non-interruption of the printing effect.

2.3.2. Rheological and Extrudability Tests

Due to the static friction between particles in the slurry, the material itself has a static yield stress (τS,i) to maintain the shape of the slurry under unloaded conditions. During 3D printing, due to the action of the extruder, the static friction between the micro-particles in the slurry is transformed into sliding or rolling friction [28]. At this time, the slurry undergoes plastic deformation, and the stress it receives is defined as dynamic yield stress (τD,i). A rheometer was used to test the rheological properties of 3DCP containing gold tailings concrete to obtain the evolution curves of static and dynamic yield stress. The static and dynamic yield stress changes with time to obtain the material's reconstruction rate (Rreco) and assemble rate (Rasse). The test process is shown in Figure 3.

Figure 3. Measurement Process of Rheological Characteristic Curves

2.3.3. Printing Height and Lateral Deformation Tests

There is a relationship between the printing height and the cross-sectional shape of the printing layer. The component with a lower printing layer height and a smaller outer contour curvature will have a significantly enhanced printing height. The relationship between the aspect ratio of the printing layer cross-section and the strength can be expressed by the strength correction coefficient [26]. When the aspect ratio is less than 1.75, that is, the ratio of the layer height to the width of the printing layer cross-section is less than 1.75, the strength correction coefficient is greater than 1.0, which can effectively maintain the stability of the component during the early printing stage. When the aspect ratio is 0.75, the strength correction coefficient approximately follows a linear relationship, and the overall data is relatively excellent. Therefore, for this experiment, when the diameter of the printing extruder head was 5mm, the corresponding layer height was 3.75mm, which could obtain excellent initial printing support performance and the printing speed of the overall component. At this time, the strength correction coefficient FAR=1.2 was used for the calculation of the later theoretical height.

Based on the above premise, a hollow cylindrical tube with a diameter of 150mm and a height of 150mm was set. When printing the model, the printing speed was set to 20mm/s, the layer height was set to 3.75mm. After calculation, the number of printing layers was 40 layers, the printing time per layer was about 24s, and the total printing time was 960s. The test process is shown in Figure 4. The maximum printing size of the printer used was 200×200×200mm. After the model printing was completed, the printing height was measured, which was the height from the printing platform to the printed model.

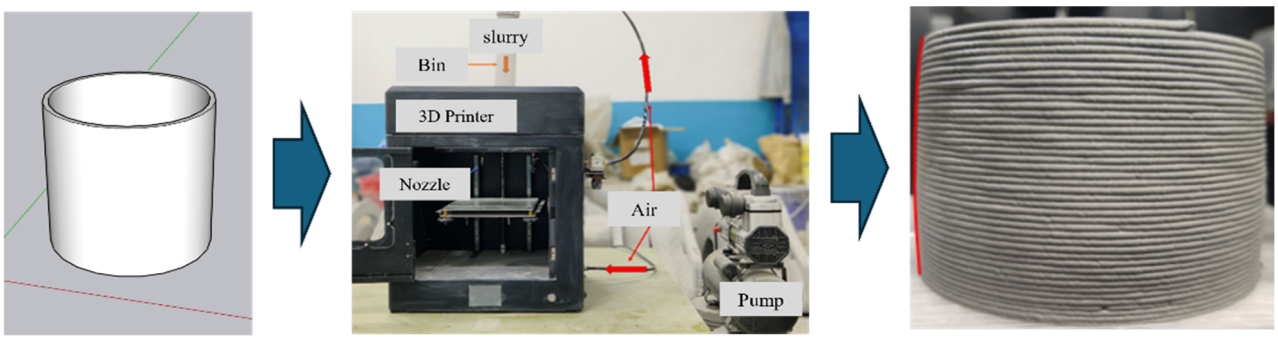

Figure 4. Test Process of Height and Lateral Deflection

There is a relationship between the printing height and the cross-sectional shape of the printing layer. Under the condition of a fixed printing height, the outer contour curvature becomes an important parameter determining the critical printing height. After printing the cylindrical model, the lateral deflection of the model was measured to determine the contribution of gold tailings after alkali activation to the height and deflection of the printing slurry.

3. Experimental Results and Analysis

3.1. Mechanical Test Results of Alkali-activated Gold Tailings Concrete

The mechanical test results are shown in Figure 5. With the gradual increase in the content of gold tailings, the 3d strength was significantly higher than that of the concrete without gold tailings. At 3d, the maximum strength of group T3 could reach 25.1MPa, which was 78.7% of its 28d strength. In contrast, the strength of group T1 ordinary concrete at 3d was only 16.2MPa, which was 56.6% of its 28d strength. From the perspective of the strength corresponding to the curing time of 7d and 28d, as the content of gold tailings gradually increased, the difference between the 7d and 28d strengths became smaller, and the strength increased faster. Adding gold tailings can rapidly increase the early strength of the slurry.

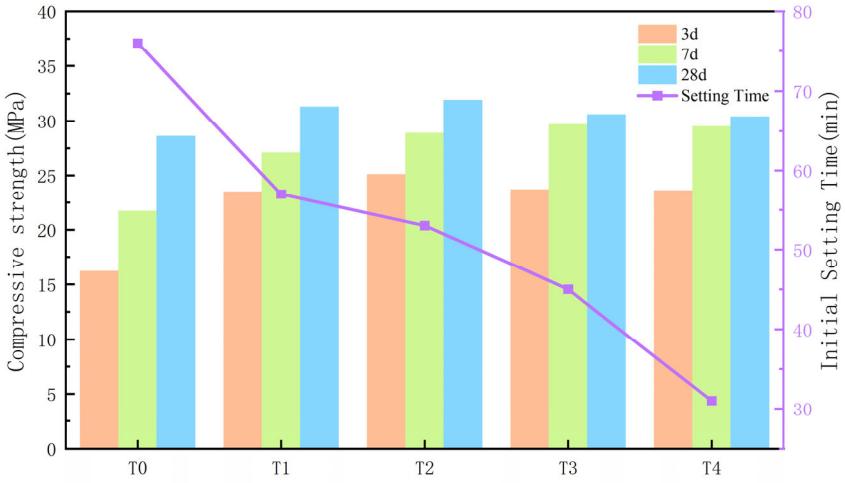

Figure 5. Compressive Strength and Setting Time of Each Group

The rapid increase in strength is due to the reaction between the alkali activator and SiO_2 and Al_2O_3 in the gold tailings. The silicon-oxygen bonds and aluminum-oxygen bonds in them work together to generate tetrahedral network aluminosilicates (N-A-S-H and C-A-S-H) gels. The reaction rate under this condition is faster than that of cement hydration. More gels can be produced in the same time, which can better promote the rapid formation of structural strength and is conducive to improving the early strength of the slurry. Higher early strength means that the lower uncured slurry of the 3D printed component can have stronger support capacity to offset the deformation caused by the load of the upper slurry, thereby increasing the printing height.

A higher initial setting time of the slurry provides a longer printing open time, while a lower initial setting time has a positive contribution to the shape retention ability of the extruded slurry. After adding gold tailings, the initial setting time of the four groups of slurries was measured using a Vicat apparatus. The results showed that the gradual increase in the content of gold tailings also promoted the gradual shortening of the initial setting time of the material. By group T4, the initial setting time had been shortened to 31min. In ordinary concrete, the initial setting of concrete is mainly due to the role of cement. During the hydration of cement to form C-S-H gel, the formed gel will hinder the unhydrated cement particles to a certain extent, thereby delaying the reaction rate of hydration. For gold tailings concrete, the alkali activator promotes the process of depolymerization-polycondensation-reconstruction of geopolymers including gold tailings. In this process, the alkali activator plays a catalytic role, prompting the aluminosilicate oligomers in the gold tailings to undergo

polycondensation reactions to form products such as calcium silicate gel, making the concrete have a faster initial setting process. At the same time, when using sodium hydroxide as the alkali activator, calcium oxide CaO in the gold tailings reacts with water to form slightly soluble $Ca(OH)_2$. Part of the calcium ions in the water neutralize charges and generate electrostatic attraction, which helps to form C-S-H gel and other products faster, further shortening the initial setting time.

3.2. Rheological and Yield Stress Evolution Curves of Alkali-activated Gold Tailings Concrete

The static yield stress parameters of the four groups of alkali-activated gold tailings concrete tested by the rheometer are shown in Table 5. the static yield stress values of each mix proportion are plotted as curves in Figure 6.

Table 5. Static Yield Stress Test Results

	τS,i (Pa)	τD,i (Pa)	Rthix (Pa/s)	Athix (Pa/s)	trf (s)
T0	2785 (1)	1362 (1)	3.56 (1)	0.30 (1)	397
T1	3976 (1.42)	1786 (1.31)	5.82 (1.64)	0.89 (2.97)	376
T2	4353 (1.56)	2063 (1.51)	6.70 (1.88)	0.94 (3.11)	342
T3	4662 (1.67)	2479 (1.82)	7.11 (1.99)	1.11 (3.66)	307
T4	5071 (-1.82)	2897 (-2.13)	8.62 (-2.42)	1.47 (-4.9)	231

For the ordinary concrete group T0, the alkali-activated concrete groups T1 to T4 showed different yield stresses. After adding gold tailings concrete, because its own particles are rougher than the replaced cement and the particle size is larger, the friction between particles is also more obvious compared with traditional cement-based concrete, thus showing higher yield stress than traditional concrete. At the same time, it can be observed that the static yield stress of group T4 increased significantly, and the slurry quickly solidified and hardened in the later stage of mixing, resulting in too short printing open time, which was no longer suitable for 3D printing. It can be determined that for alkali-activated gold tailings concrete, the activation process has a significant impact on the thixotropic properties, and the alkali activation can greatly increase the yield stress of the slurry. However, it should be noted that when the content of gold tailings is too large, the friction between particles and the van der Waals force generated by ions in free water due to alkali activation cause the fluidity of the slurry to exceed the range that 3D printing can afforded, leading to phenomena such as short printing open time and poor printing effect in group T4.

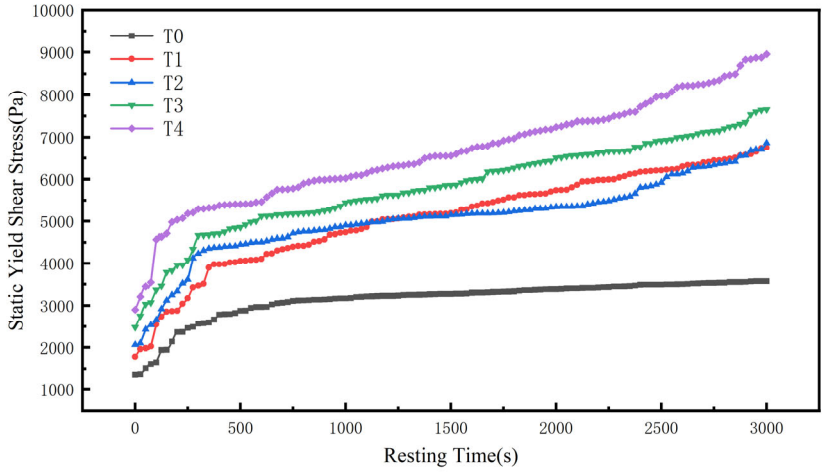

Figure 6. Yield Stress Evolution Curves

In terms of reconstruction rate and assemble rate, it can be seen that T0's reconstruction rate is much lower than that of concrete mixed with gold tailings, which has a negative effect on the printing bearing capacity of 3D printing slurry. A lower reconstruction rate means that a lower printing speed is required to ensure the quality of the printed component. The reconstruction rates of groups T1 to T4 are higher, which can endow the lower slurry of the model with higher support strength during the printing process, ensuring the printing height and printing speed. The assemble rates of groups T1 to T4 are also relatively high, which can obtain the strength of the slurry after hardening faster and ensure the structural stability of the model itself.

The gold tailings content of groups T1 and T2 is more suitable for 3D printing. Since the reconstruction rate and assemble rate of group T1 are smaller than those of group T2, the printing open time of the material is also longer, which is more suitable for the use of printed components with lower

overall height but larger volume. Group T2, on the contrary, is suitable for printing models with higher printing height and shorter required printing time, that is, the material is selected according to the printing time of the model.

3.3. 3D Printing Height and Lateral Deformation Performance of Alkali-activated Gold Tailings Concrete

During 3D printing, the fluidity and printing height basically show an inverse relationship. Slurry with lower fluidity has a higher printing height. For 3DCP technology, because the extruder will generate shear force on the slurry during operation, the lower the fluidity of the slurry, the more difficult the extrusion printing process will be, leading to inconsistent extrusion of the printing strip and poor printing quality. Figure 7 shows the corresponding relationship between fluidity and printing height of groups T0 to T5.

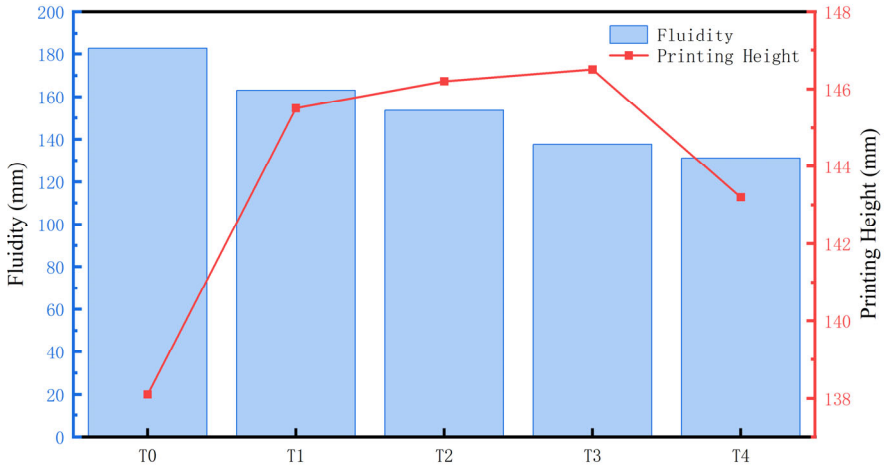

Figure 7. Fluidity and Printing Height Test Results

After replacing part of the cement with gold tailings and adding an alkali activator, the fluidity decreased from 182.6mm of the gold tailings-free group T0 to 146.2mm. With the gradual addition of gold tailings, the fluidity also gradually decreased. At the same time, compared with the ordinary 3DCP concrete without tailings, the fluidity of the concrete mixed with gold tailings decreased significantly. Due to the high modulus of the selected sodium silicate liquid reagent, its viscosity is also relatively high, which contributes to the cohesiveness of the concrete mixing. Secondly, the activated gold tailings have more angular microstructures, and the friction between particles also makes the fluidity of gold tailings concrete weaker than that of traditional concrete to a certain extent. A reasonable decrease in fluidity is conducive to maintaining the printing height of 3D printed components, that is, the components are less likely to deform and collapse under the action of gravity, and it is also conducive to reducing detail loss and shape distortion caused by excessive flow, improving printing accuracy.

The printing height of 3DCP is determined by the printing speed, the initial rheological properties of the slurry, and the strength. Due to the lower fluidity after mixing gold tailings, the printing height of the model increased from 138.1mm to a maximum of 146.6mm. The final stable height of the model increased slightly. Compared with the theoretical height of the model of 150mm, the deformation was 3.3%, which was within the 5% deformation range and within a reasonable deformation range during the actual printing process.

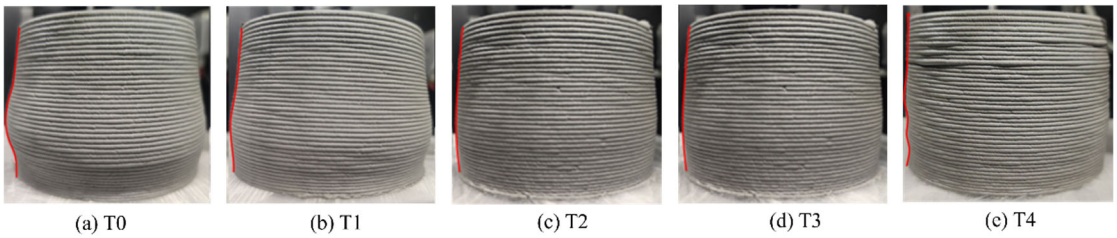

Figure 8. Model Printing Height and Lateral Deflection Changes Under Different Mix Proportions

With the improvement of the printing height retention ability, the lateral deflection of the component also decreases. The actual test lateral deformation is shown in Figure 8. Due to the action of gravity, the upper slurry generates a load on the lower uncured slurry of the model, resulting in plastic deformation. For traditional concrete, because its initial setting time is longer than that of gold tailings concrete, the deformation of the lower slurry is more serious, and the maximum lateral deflection point is about 1/3 of the overall structure. Compared with traditional concrete, the gold tailings concrete has lower fluidity and static yield stress, and the strength of the slurry forms faster after extrusion, resulting in less lateral deformation of the lower part. It can be seen from Figure 8 that the shape retention of alkali-activated gold

tailings concrete is better than that of traditional concrete, indicating that after mixing gold tailings and activation, the overall fluidity of the concrete can be effectively improved, making it more suitable for 3DCP technology. In group T4, the lower part of the slurry was deformed because the concrete had poor extrusion during printing, which affected the overall printing appearance quality and height. That is, the lower workability of the slurry will affect the 3D printing effect.

4. Conclusion

(1) After replacing part of the cement in the concrete with gold tailings and conducting alkali activation treatment, the mechanical strength of the concrete increases faster than that of traditional concrete. The 28-day strength of groups T1 to T4 is increased to varying degrees compared with group T0, and the growth rate of the early strength at 3d and 7d is also faster than that of group T0. The initial setting time is shorter, which is beneficial to the shape retention ability of the lower slurry of the model during 3D printing.

(2) In terms of rheology, groups T1 to T4 containing gold tailings have a faster growth rate of yield stress compared with group T0, which has a positive contribution to maintaining the 3D printing height. However, the yield stress growth rate of group T4 is too fast, which is prone to extrusion difficulties and other phenomena.

(3) Groups T1 and T2 showed more excellent effects in 3D printing. The printing open time and printing height of the two groups can coexist effectively. From the perspective of printing effect, the apparent characteristics of groups T1 and T2 are better than those of group T4.

Acknowledgment

We extend our sincere gratitude to Ms. Li Huiting for providing experimental instruments and materials for rheological measurements and mechanical characterization analysis, as well as offering valuable guidance on rheological analysis.

References

[1] SARI M, YILMAZ E, KASAP T. Long-term ageing characteristics of cemented paste backfill: Usability of sand as a partial substitute of hazardous tailings[J]. Journal of Cleaner Production, 2023, 401: 136723.

[2] WANG Kun, ZHANG Zheng, KAREN A. HUDSON-EDWARDS, et al. Characteristics, disasters, and resource potential of tailings[J]. Metal Mine, 2024, (08): 216-227. DOI:10.19614/j.cnki.jsks.202408029.

[3] SHI Canhai, LIU Mingsheng, CHENG Lijia, et al. Research progress and engineering practice in comprehensive utilization of tailings[J]. China Mining Magazine, 2024, 33(02): 107-114.

[4] SU Peijun, WANG Shuyun, WANG Fan, et al. Study on component proportion of large-amount gold tailings sintered clay bricks[J]. Municipal Engineering Technology, 2024, 42(11): 47-52. DOI:10.19922/j.1009-7767.2024.11.047.

[5] ZHAO Yingliang, XING Jun, LIU Hui, et al. Preparation of filling cementitious materials by alkali melting activation of tailings from Canzhuang Gold Mine[J]. Nonferrous Metal Engineering, 2017, 7(06): 80-85.

[6] Boboev I R, Kholikzoda T, Sel'nitsyn R S, et al. Material composition and diagnostic leaching tests of gold mine tailings dump (Taror deposit, Tajikistan)[J]. Metallurgist, 2024: 1-9.

[7] Ren B, Zhao Y, Bai H, et al. Eco-friendly geopolymer prepared from solid wastes: A critical review[J]. Chemosphere, 2021, 267: 128900.

[8] DENG Peng, ZHONG Hao, GUO Shuaicheng. Chemical-high temperature-mechanical composite activation of gold tailings and mechanism analysis[J]. Journal of Hunan University (Natural Sciences), 2023, 50(09): 79-87. DOI:10.16339/j.cnki.hdxbzkb.2023104.

[9] Song Q, Zou Y, Bao J, et al. Disposal of solid waste as building materials: A study on the mechanical and durability performance of concrete composed of gold tailings[J]. Journal of Materials Research and Technology, 2024, 30: 2111-2124.

[10] MAO Yufei, GUO Zenghui, CHEN Hui, et al. Research progress on reinforcement technology of 3D printing concrete[J]. Bulletin of the Chinese Ceramic Society, 2024, 43(05): 1557-1568. DOI:10.16552/j.cnki.issn1001-1625.2024.05.003.

[11] Chang Z, Liang M, Xu Y, et al. 3D concrete printing: Lattice modeling of structural failure considering damage and deformed geometry[J]. Cement and Concrete Composites, 2022, 133: 104719.

[12] Yang L, Gao Y, Chen H, et al. 3D printing concrete technology from a rheology perspective: a review[J]. ADVANCES IN CEMENT RESEARCH, 2024.

[13] Khan S A, Koç M. Buildability analysis of 3D concrete printing process: a parametric study using design of experiment approach [J]. Processes, 2023, 11(3): 782.

[14] Jayathilakage R, Rajeev P, Sanjayan J. Rheometry for concrete 3D printing: a review and an experimental comparison[J]. Buildings, 2022, 12(8): 1190.

[15] de Matos P R, Zat T, Lima M M, et al. Effect of the superplasticizer addition time on the fresh properties of 3D printed limestone calcined clay cement (LC3) concrete[J]. Case Studies in Construction Materials, 2023, 19: e02419.

[16] Kondepudi K, Subramaniam K V L, Nematollahi B, et al. Study of particle packing and paste rheology in alkali activated mixtures to meet the rheology demands of 3D Concrete Printing[J]. Cement and Concrete Composites, 2022, 131: 104581.

[17] ZHU Chunhong, ZHOU Kai, HE Lei. Study on mechanical properties of 3D printed gold tailings sand ultra-high performance concrete[J]. Metal Mine, 2023, (10): 259-264. DOI:10.19614/j.cnki.jsks.202310036.

[18] Zhang H, Cao S, Yilmaz E. Polymer shape effect on damage evolution, internal defects and crack propagation of 3D-printed polymer-based cementitious backfill[J]. Construction and Building Materials, 2023, 406: 133386.

[19] Ma H, Yang Z, Li Q, et al. STUDY ON THE PREPARATION OF GEOPOLYMERS FROM COPPER TAILINGS[J]. FEB-FRESENIUS ENVIRONMENTAL BULLETIN, 2022: 9464.

[20] Nunes G M, Anjos M A S, Lins A B S M, et al. Evaluation of the mechanical behaviour of representative volumetric elements of 3DCP masonry mixtures with partial replacement of cement by limestone filler and metakaolin[J]. Journal of Building Engineering, 2023, 78: 107650.

[21] WU Xikai, SHI Qingxuan, ZHAO Yu. Research progress on rheology and printability of 3D printing concrete[J/OL]. Journal of Xi'an University of Architecture and Technology (Natural Science Edition), 1-11 [2024-11-17]. http://kns.cnki.net/kcms/detail/61.1295.TU.20240704.1631.002.html.

[22] Davidovits J. Geopolymers and geopolymers new materials[J]. Journal of Thermal Analysis, 1989, 35(2): 429.

[23] WANG Changjun, HU Zhigang, XU Dandan, et al. Study on rheological and mechanical properties of cement grouting material prepared from gold tailings sand[J]. Metal Mine, 2023, (07): 283-290. DOI:10.19614/j.cnki.jsks.202307036.

[24] Jayathilakage R, Rajeev P, Sanjayan J G. Yield stress criteria to assess the buildability of 3D concrete printing[J]. Construction and Building Materials, 2020, 240: 117989.

[25] Shahzad Q, Li F. An innovative method for buildability assessment of 3d printed concrete at early-ages[J]. Construction and Building Materials, 2023, 403: 133167.

[26] Roussel N. A thixotropy model for fresh fluid concretes: Theory, validation and applications[J]. Cement and concrete research, 2006, 36(10): 1797-1806.

[27] Kruger J, Zeranka S, van Zijl G. 3D concrete printing: A lower bound analytical model for buildability performance quantification[J]. Automation in Construction, 2019, 106: 102904.

[28] Alexandridis A, Gardner N J. Mechanical behaviour of fresh concrete[J]. Cement and Concrete Research, 1981, 11(3): 323-339